

Fellenius, B.H. 2012. Critical assessment of pile modulus determination methods. Discussion. Canadian Geotechnical Journal, 49(5) 614-621.

## Discussion of “Critical assessment of pile modulus determination methods”<sup>1</sup>

Bengt H. Fellenius

Lam and Jefferis (2011) have produced a timely, well written, and worthy paper. I would like to add a few comments to the authors' presentation of the strain measurements. Moreover, the authors' recommendations regarding the *E*-modulus to be used for determining the load distribution in a pile subjected to a static loading test from the strain measurements need both to be emphasized and moderated, which is what the following brief compilation of case records aims to do.

The authors' paper presents the changes of strain of up to 100+  $\mu\epsilon$  in the pile occurring as a result of the concreting and during the set-up time between pile construction and the static loading test. I think it is worthwhile to emphasize that the changes are caused by three different processes: temperature change (heating and cooling), swelling of the concrete, and reconsolidation by the soil (Fellenius et al. 2004). First, changes of strain are imposed during the hydration process as a consequence of the differences in thermal response between the concrete and the steel (in the sister bar gages). The hydration process causes an increase of temperature, which takes place over several hours, about 24 h rather than the 3 h the authors report. At first, the concrete is fluid, and there is very little strain or stress transferred between the concrete and the sister bars. Second, when the concrete starts to harden, bonding develops between the rebars and the concrete, and a further temperature increase will result in an apparent elongation — tension — of the rebars. During the subsequent cooling, which can take weeks or months, the concrete (usually) reduces more than the rebars, manifested by a shortening of the rebars — apparent compression — co-occurring with tension in the concrete. During the following period, the concrete absorbs water from the soil, which results in a volume increase — swelling — recorded as a rebar elongation — apparent tension — and, conversely, compression in the concrete. Third, at depth, when the soil recovers from the disturbance imposed by the construction, it usually tends to settle, which causes negative direction shear forces to develop, resulting in an increase of load in the pile — noticeable as residual load, which the authors showed

to have taken place for the subject pile. Consequently, when the static loading test commences, a state of stress and strain exists in the pile that to some extent will affect the response to the applied load increments, as registered by the strain gages. The evaluation of the strain-gage records, in particular when the secant stiffness method is applied, needs to consider this, as suggested for a few of the following case histories.

### Case 1

Bradshaw et al. (2012) report results from a 1.83 m diameter, open-toe, strain-gage instrumented, driven, steel pipe pile with a 38 mm thick wall. The pile was not concreted. The uppermost strain-gage level was 1.8 m (1.0 pile diameter) below the pile head and 1.2 m below the ground surface. The static loading test was a quick test with 23 equal increments of 1100 kN applied every 10 min to a maximum load of 25 500 kN, when bearing failure developed. The loads were measured using a separate load cell. Figure 1 presents the secant and tangent stiffness curves for the uppermost strain-gage level.

As could be expected, both methods of determining the pile stiffness give practically the same pile stiffness, a constant value of 46 GN, which when divided by the total steel area is about equal to the *E*-modulus of steel (about 200 GPa). The scatter of values in the tangent stiffness diagram shows, as also mentioned by the authors, that the differentiation process of the tangent stiffness method is more sensitive to inaccuracies of load and strain measurements, as opposed to the secant stiffness method. However, with a sufficient number of data points, the inaccuracies even out and the average stiffness is essentially the same for both methods when applied to this steel pile.

### Case 2

A 400 mm (16 inch) diameter, 18.5 m long, strain-gage instrumented continuous flight augercast (CFA) test pile was constructed on 26 April 2011, near Edmonton, Alberta, and subjected to a static loading test 13 days later. The cage consists of five 20 mm diameter reinforcing bars and a 9 mm diameter spiral reinforcement at 230 mm spacing (rise). Total area of reinforcement was about 16 cm<sup>2</sup>. The uppermost strain-gage level was 1.6 m (4.0 pile diameters) below the pile head and 1.5 m below the ground surface. The static loading test was a quick test with 19 increments of about 100 kN applied every 10 min to a maximum load of

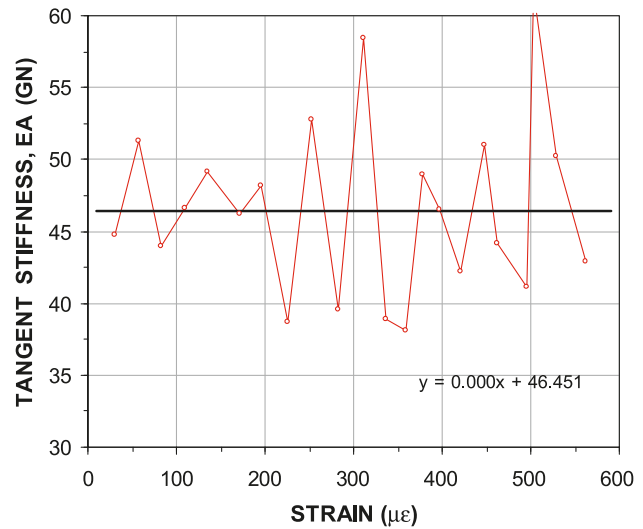
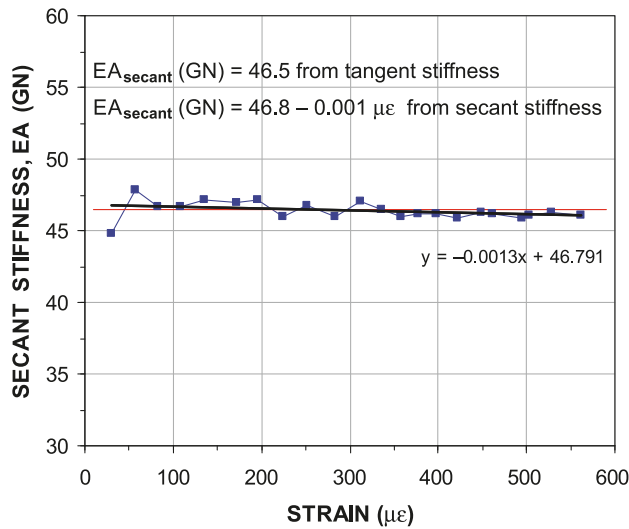
Received 28 December 2011. Accepted 27 January 2012.  
Published at [www.nrcresearchpress.com/cgj](http://www.nrcresearchpress.com/cgj) on 30 April 2012.

**B.H. Fellenius.** 2475 Rothesay Avenue, Sidney, BC V8L 2B9, Canada.

**E-mail for correspondence:** [Bengt@Fellenius.net](mailto:Bengt@Fellenius.net).

<sup>1</sup>Appears in the Canadian Geotechnical Journal, **48**(10): 1433–1448 [doi: 10.1139/t11-050].

**Fig. 1.** Case 1. Pile stiffness for a 1.83 m diameter steel pile (data from Bradshaw et al. 2012).



1800 kN, when reaction support gave indication of failing, and the test was terminated. The loads were measured using a separate load cell. Figure 2 presents the secant and tangent stiffness curves for the uppermost strain-gage level.

Also for case 2, the two methods provide similar results. The tangent stiffness method displays a smaller scatter than was shown for case 1. The data do not show any appreciable influence of stress level. The evaluated stiffness, 2600 MN, corresponds to a concrete  $E$ -modulus of 20 GPa. That this value is low is probably due to the short hydration time.

### Case 3

Fellenius et al. (2004) reports results of static loading tests on a 400 mm (16 inch) diameter, 46 m long, strain-gage instrumented, concreted, steel pipe pile. The instrumentation cage consisted of two U-bars, each with a 7.8 cm<sup>2</sup> cross section. The uppermost strain-gage level was 1.3 m (3.2 pile diameters) below the pile head and 0.4 m below the ground surface. The static loading test was a quick test with 13 increments of about 150 kN applied every 10 min to a maximum load of 1900 kN, when the pile failed by plunging. The loads were measured using a separate load cell. Figure 3 presents the secant and tangent stiffness curves for the uppermost strain-gage level.

The stiffness values are consistent and there is practically no difference between the two methods for determining the pile stiffness. At first, the secant stiffness values deviate from the trend line, which is probably due to the pile cross section initially not being uniformly stressed, which conflicts with the assumption of uniform (plane) stress distribution across the pile cross section. After a few increments of load, at an imposed strain of about 100  $\mu\epsilon$ , the influence of the initial deviation from the assumed condition becomes relatively smaller, the stiffness line can develop, and the Saint-Venant's principle, referred to by the authors, can set in. The differentiation of the tangent stiffness method eliminates the influence of this and displays, therefore, the stiffness line also at the initially smaller strain values. The stiffness,  $EA$ , does not change much with increasing strain. At a strain of 150  $\mu\epsilon$ , the stiffness is about 6.6 GN. Proportioning this for the amount

of steel and concrete involved, the value corresponds to an  $E$ -modulus of 24 GPa.

### Case 4

A static loading (CH2M Hill 1995) was carried out on a 600 mm diameter, octagonal, 33 m long, driven, prestressed concrete pile reinforced with sixteen 12.7 mm (0.5 inch) strands with a total strand area of 16 cm<sup>2</sup> (2.45 in<sup>2</sup>). The net pile cross section was 0.303 m<sup>2</sup>. The nominal concrete cylinder strength was 45 MPa. Two parallel systems of strain gages were installed in the pile: electrical resistance gages and vibrating wire gages. The uppermost strain-gage level was 1.5 m (2.5 pile diameters) below the pile head and 1.0 m below the ground surface. The static loading test was a quick test with 27 increments of about 150 kN applied every 15 min to a maximum load of 3800 kN, at which load the pile reached bearing failure. The loads were measured using a separate load cell. The results of the two strain-gage types were almost identical. Figure 4 presents the secant and tangent stiffness curves for the uppermost strain-gage level. The plotted values are from both types of gages.

Apart from the strain values lower than about 150  $\mu\epsilon$ , the two methods again give practically identical results. The secant stiffness portion before 100  $\mu\epsilon$  reduces progressively with increasing strain as if following an exponential curve similar to that for case 3, but after a few increments of load the cross section appears to be stressed uniformly and the linear trend appears. As shown in Fig. 4, adjusting the strain records by adding 20  $\mu\epsilon$  to each value removes the initial gradual reduction appearance, and the secant stiffness line becomes essentially straight, confirming the secant line determined by the tangent stiffness method.

### Case 5

A 900 mm diameter, 19 m long, strain-gage instrumented bored pile was constructed in a weathered limestone (Geo Optima Pt. 2011). The measured 28 day concrete cylinder strength was 37 MPa. The pile was reinforced with a steel cage made up of fourteen 22 mm diameter reinforcement

Fig. 2. Case 2. Pile stiffness for a 400 mm CFA pile.

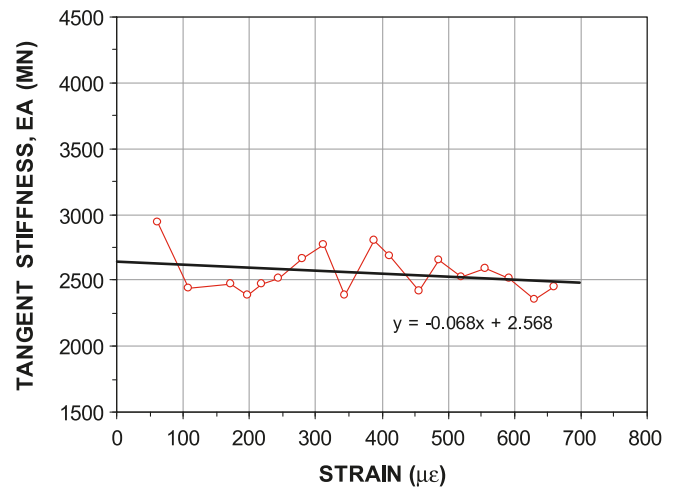
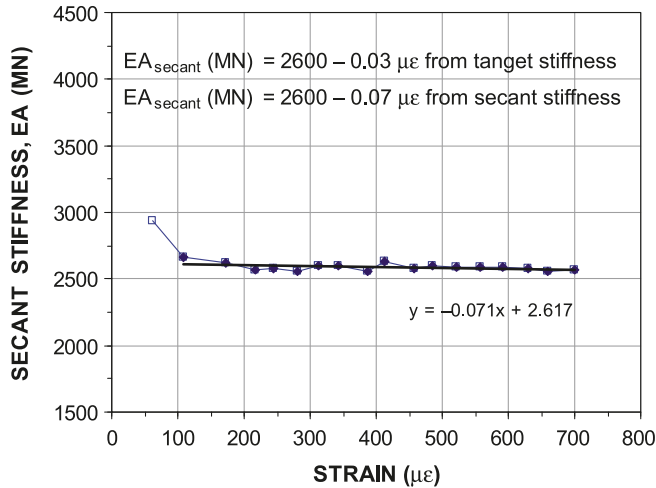


Fig. 3. Case 3. Pile stiffness for a 600 mm concreted pipe pile (data from Fellenius et al. 2004).

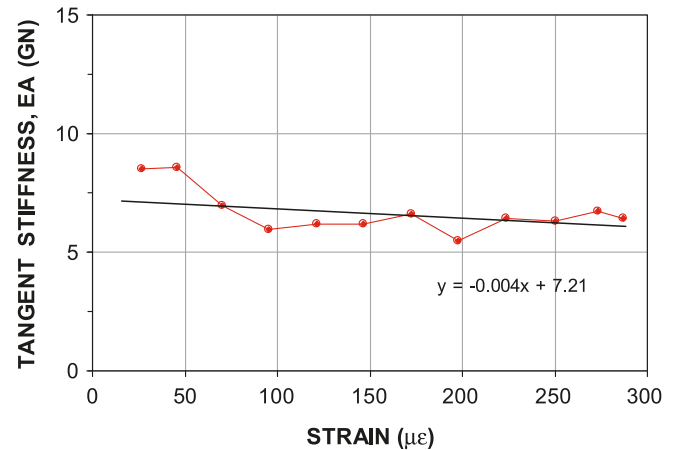
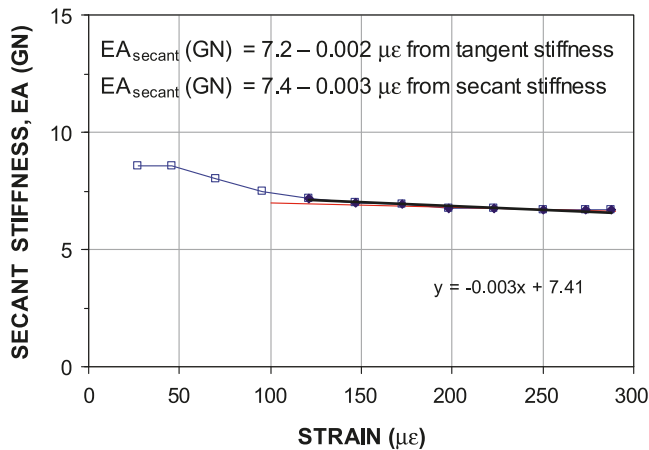
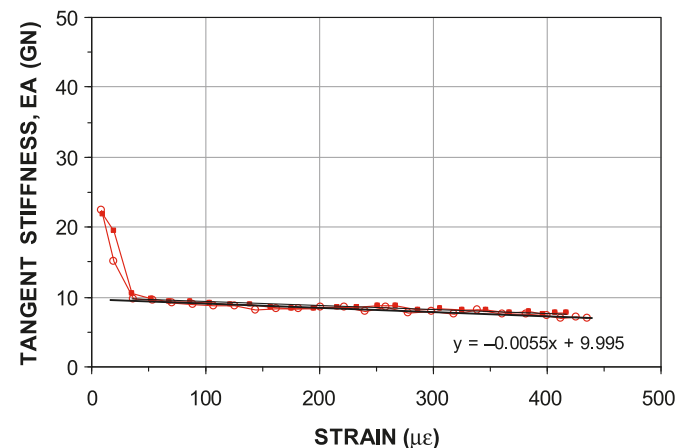
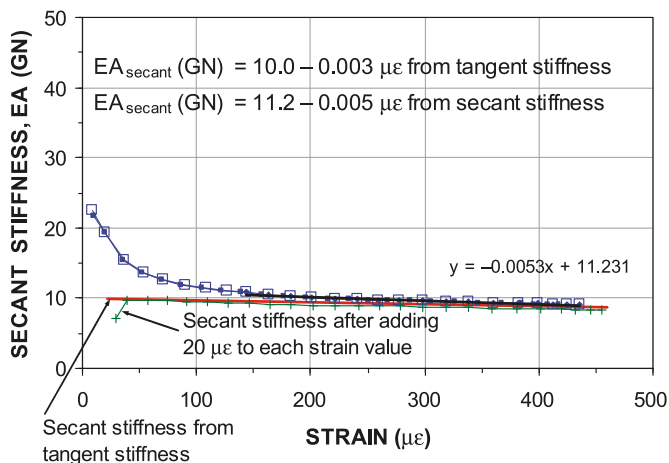


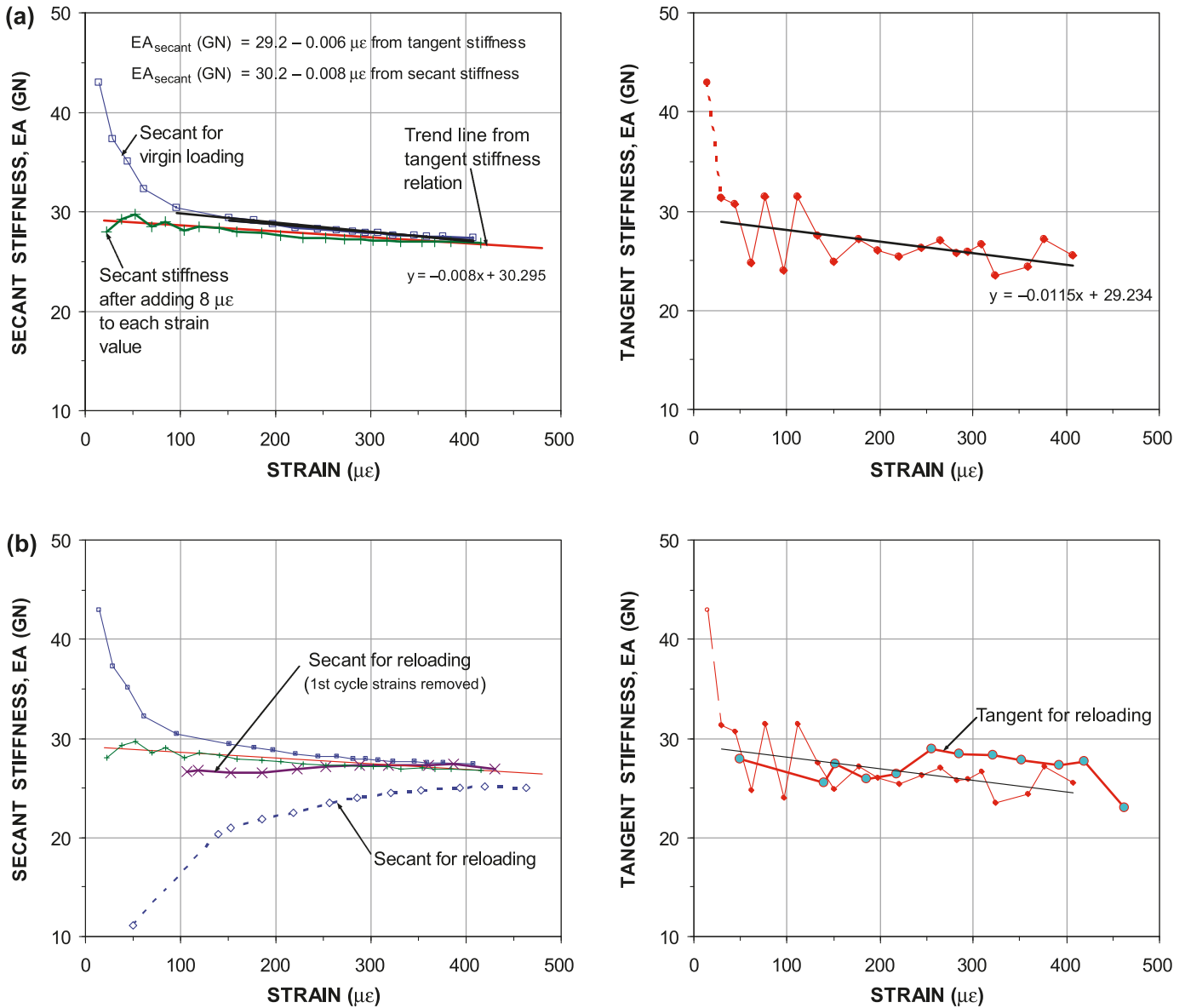
Fig. 4. Case 4. Pile stiffness for a 600 mm diameter prestressed pile (data from CH2M Hill 1995).



bars. The instrumentation consisted of vibrating-wire strain gages. The uppermost strain-gage level was 2.0 m (2.2 pile diameters) below the pile head. The shaft resistance above the gage level had been removed by excavating the soil to the depth of the gage level. The static loads were applied by means of two jacks and the applied load was recorded separately for each jack by means of a load cell. The static load-

ing test was a quick test with 24 increments of about 500 kN applied every 10 min to a maximum load of about 12 000 kN; the maximum capacity of the loading system. After unloading, the pile was reloaded to the same load using 14 increments of about 800 kN, also applied every 10 min. Figure 5a presents the secant and tangent stiffness curves for the uppermost strain-gage level for the virgin loading.

**Fig. 5.** Case 5: (a) pile stiffness for a 900 mm bored pile (data from Geo Optima Pt. 2011); (b) pile stiffness values of the reloading event added to the virgin loading values (data from Geo Optima Pt. 2011).



Again, apart from the first series of increments, the secant and tangent method curves are quite similar. As in case 4, for the first series of increments, the secant stiffness method shows values that appear to follow an exponentially diminishing trend. However, by adding a small value, a mere 8  $\mu\epsilon$ , to each recorded value of strain, the secant stiffness curve changes to a line that is almost identical to the secant stiffness line determined by the tangent method.

In Fig. 5b, the stiffness values from the reloading are added to the virgin test values (first cycle). While the tangent stiffness values for the reloading do not differ that much from those of the virgin loading, the secant stiffness values deviate considerably. (The secant stiffness values are determined using the same zero value — start value — as used for the plot of the virgin values — first cycle). When treating the reloading as a stand-alone event with the strain value immediately before loading (30  $\mu\epsilon$ ) set as zero and all strain

values indicated as changes from that start, a secant stiffness line emerges that is reasonably close to the tangent stiffness line. Obviously, the unloading–reloading changed the “spring” response of the pile. It is probable that had the reloading continued beyond the maximum load of the virgin loading, then both stiffness plots would have developed to show trends very close to that for the secant and tangent virgin lines. The observation demonstrates the significant influence on the stiffness response caused by including unloading–reloading cycles in a test.

**Case 6**

Fellenius and Tan (2010) report results of a static loading test on a strain-gage instrumented 1200 mm diameter, 37 m long bored pile. The instrumentation cage consisted of two U-bars with a 7.8 cm<sup>2</sup> cross section. The uppermost strain-

gage level was 2.25 m (1.9 pile diameter) below the pile head and 1.75 m below the ground surface. The pile was constructed with an O-cell placed at the pile toe. No permanent casing was used.

The test programme consisted of four loading events — four cycles: an initial head-down test, cycle 1; an O-cell test, cycle 2; a repeat head-down test, cycle 3; and a repeat O-cell test, cycle 4. Unfortunately, the head-down reaction arrangement included a main beam that was too light. When this was discovered during cycle 1a, the test was interrupted to attempt to improve the beam stiffness, but the resumed loading, cycle 1b, showed this to have been unsuccessful. The upward movement of the reaction beam above the jack was several times larger than the downward movement of the pile head. Therefore, the two head-down cycles could not be carried to as high a load as had been planned for.

The three loading cycles — 1a, 1b, and 3 — consisted of 12, 15, and 18 increments of about 1000, 1300, and 1000 kN, respectively, applied every 10 min. The loads were measured using a separate load cell. Figure 6a presents the secant and tangent stiffness curves for the uppermost strain-gage level.

Neither the secant nor the tangent stiffness relations from cycle 1a show definite trends. The trends implied by the dashed lines have very little credibility. The relations for cycles 1b and 3 have been added as shown in Fig. 6b, but this does not make the results case any clearer. The tangent stiffness diagram includes the tangent stiffness line determined from cycle 2 for the gage response nearest the O-cell. However, the seemingly good agreement between this line and the one from the uppermost gage could be coincidental. The cause of the erratic stiffness response is considered to be the large stress variations at the pile head when the main reaction beam adjusted to its upward movement. (The tangent stiffness response of the gage level nearest the O-cell was used for the evaluation of the pile response to load).

### Case 7

Kim et al. (2011) report results of a static loading test on a strain-gage instrumented 600 mm diameter, 33 m long, driven, prestressed cylinder pile with a 120 mm wall thickness. The pile was cast with a series of vibrating wire gages and access cables embedded in the pile wall. The uppermost strain-gage level was 1.2 m (2.0 pile diameters) below the pile head and about level with the ground surface. The static loading test was a quick test with 33 increments of about 200 kN applied every 10 min to a maximum load of about 6500 kN. The loads were measured using a separate load cell. Structural failure developed at the pile head when the maximum load was being applied. Figure 7 presents the secant and tangent stiffness curves for the uppermost strain-gage level.

The tangent stiffness line develops from the very first value and is consistent until the onset of structural failure starts to interfere with the strain development. In contrast, the secant stiffness line diminishes exponentially, and this over the entire length of the records until the failure started to develop. By simply adding a constant strain value of  $87 \mu\epsilon$  to the recorded strain and determining the secant stiffness relation from these new strain values, a line emerges that

is essentially linear except for the first value and very close to the secant stiffness line determined in the tangent stiffness method. Why  $87 \mu\epsilon$ ? Well, this is the value that happens to result in the straight line. There is no other direct reason for picking just this value and no other value. However, the  $87 \mu\epsilon$  value is in the range of the strain changes that took place for this pile between the driving and the loading test 166 days later. These changes were recorded: the change of strain in the uppermost gage from before the driving to the end of driving indicates an about  $50 \mu\epsilon$  lengthening of the reinforcement. Between driving and the loading test, a further about  $200 \mu\epsilon$  lengthening occurred. The cause is probably swelling of the concrete in absorbing water from the soil. Note that as the swelling pulls the reinforcing bars along (along with the sister bar vibrating wire gages), the bars also resist the lengthening, which leaves the concrete in a corresponding compressed state. (The phenomenon of changes of strain between concrete and reinforcing steel at this site has been discussed by Fellenius et al. 2009 and Kim et al. 2011).

Not knowing the absolute state of strain for either material, all one can say for certain is that strain changes occurring before the test will have some effect on how the pile cross section later reacts to outside forces. The secant stiffness method incorporates whatever strains there are in the pile and their relative effect becomes smaller as the imposed strain increases, which is causing the apparent exponential development of the secant stiffness. The differentiation approach of the tangent stiffness method is affected by this to a much smaller extent.

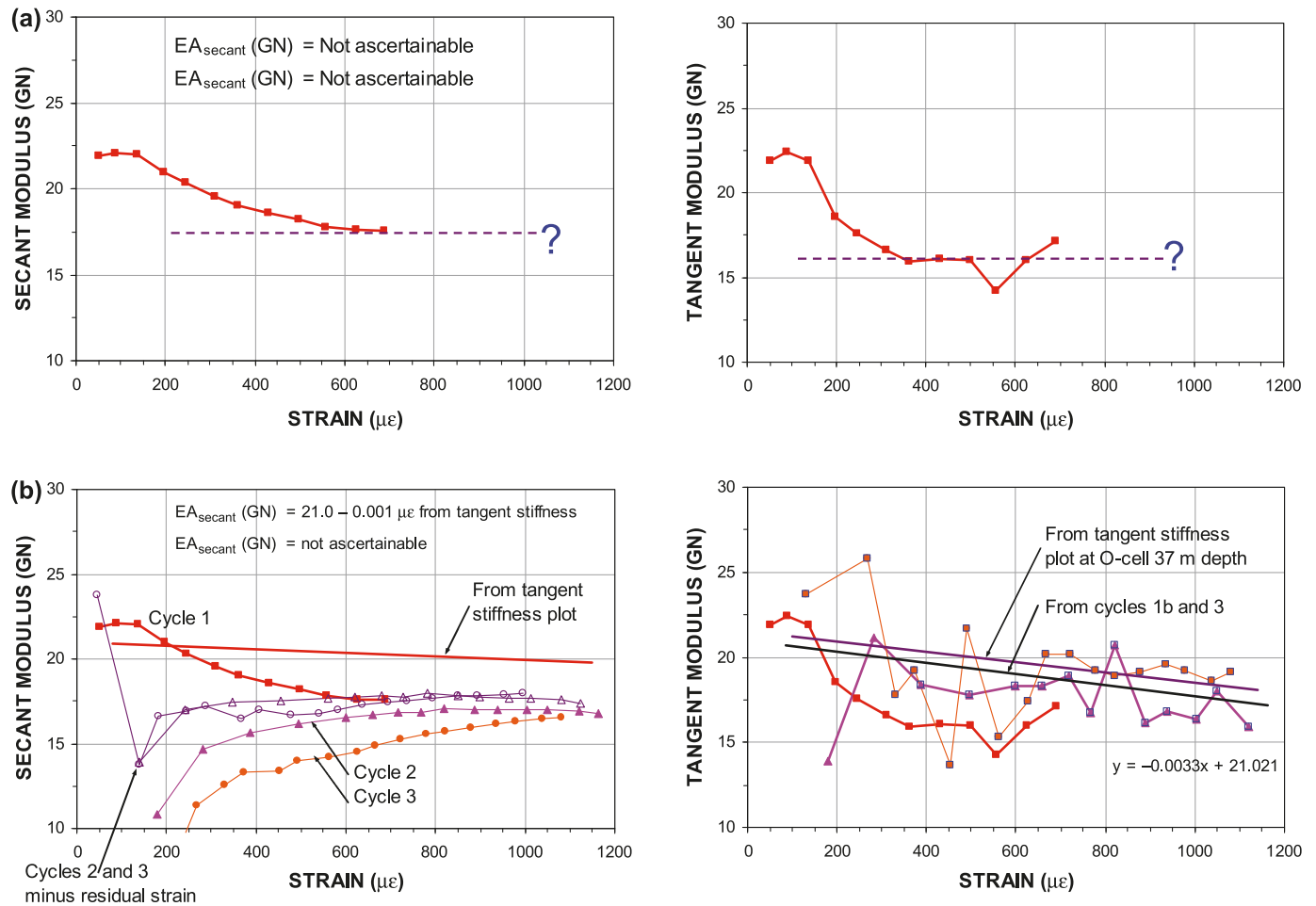
### Case 8

The case record presented as case 7 is not truly representative of a “real” pile as it was a special test pile. Although manufactured in a spun-pile plant, it could not be prestressed because the prestressing arrangement would have damaged the gage cables. However, the project described by Kim et al. (2011) also included a standard 600 mm diameter spun pile with a 85 mm thick wall, driven to 56 m depth, and the results of that test are as follows.

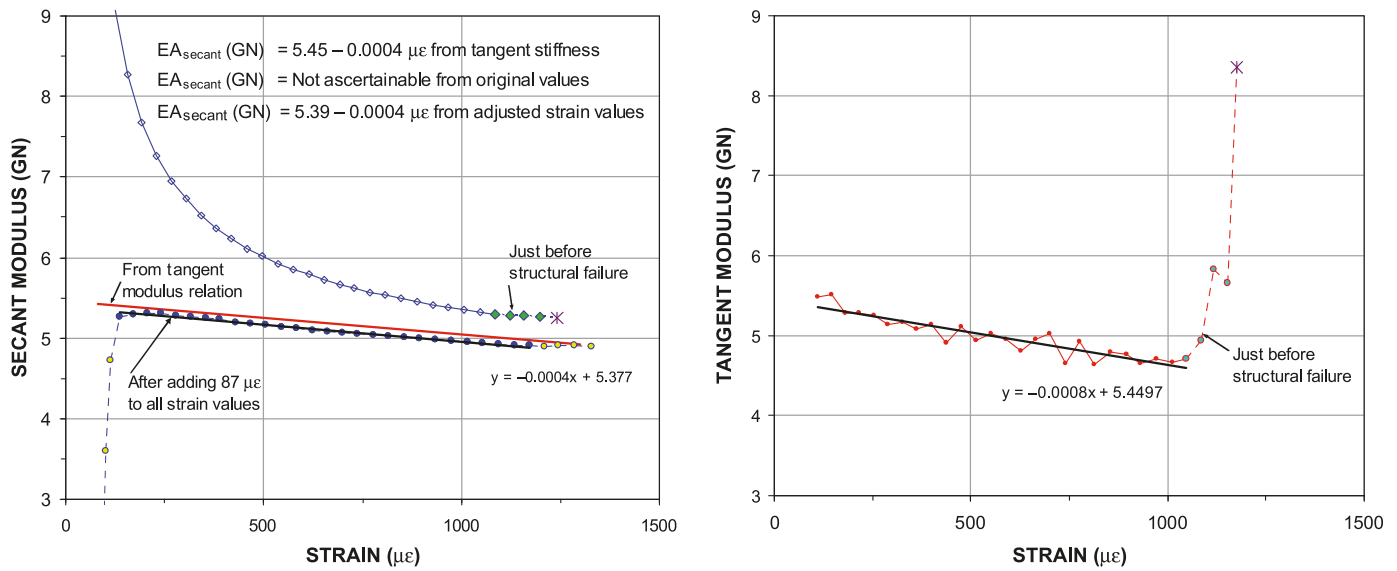
The uppermost strain-gage level was 2.0 m (3.3 pile diameters) below the pile head and about 1.0 m below the ground surface. The inside of the concrete cylinder was grouted and the gages were attached to a reinforcing cage lowered into the grout. The static head-down loading test, performed after a 6 month wait, was a quick-method test carried out after an initial O-cell test (that did not move the pile head). The test programme included applying load increments of 300 kN every 10 min until plunging failure occurred. At the 27th increment, when the applied load was 8300 kN, a valve in the jack pumping system sprung a leak and the pile had to be unloaded. In reloading after repairs had been made, load increments of 500 kN were used and at the 17th increment, when the applied load approached 9000 kN, plunging failure developed. Figure 8a presents the secant and tangent stiffness curves for the uppermost strain-gage level, showing secant stiffness lines determined from the two methods to be practically identical. That the pile underwent similar swelling strains as the case 7 pile is not reflected in the lines.

Figure 8b shows the stiffness lines from the reloading of the pile, cycle 2. The tangent stiffness line is quite similar to

**Fig. 6.** Case 6: (a) pile stiffness for a 1000 mm bored pile during cycle 1a (data from Fellenius and Tan 2010); (b) pile stiffness for the 1000 mm bored pile during cycles 1a, 1b, and 3 (data from Fellenius and Tan 2010).



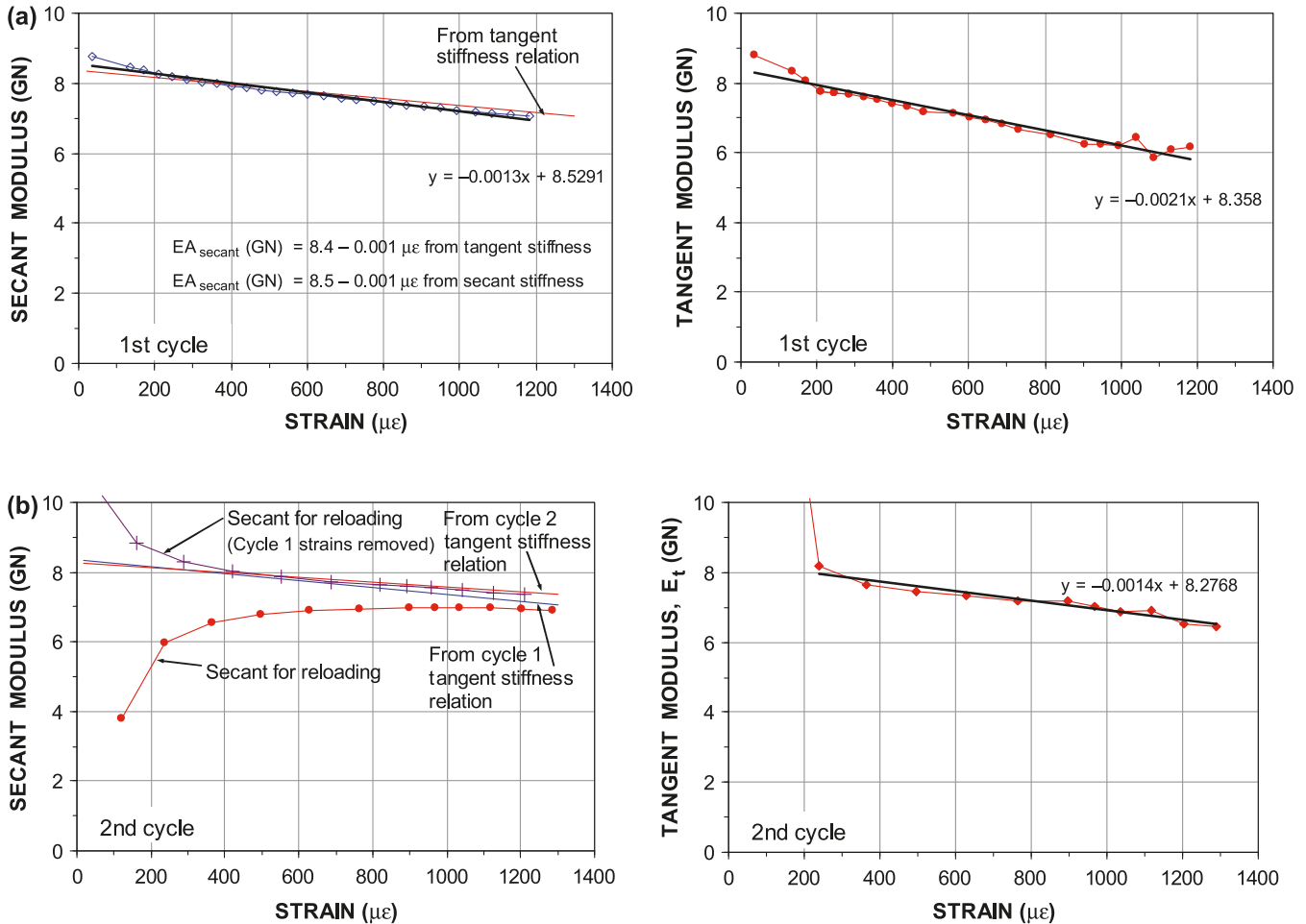
**Fig. 7.** Case 7: pile stiffness for a 600 mm diameter concrete cylinder pile (data from Kim et al. 2011).



that of the virgin loading. However, the secant stiffness line shows a response similar to that for the reloading in case 5: the stiffness increases at a reducing rate until toward the end it gets close to the secant line determined in the tangent stiff-

ness method. When the secant stiffness was determined for strains that disregarded the strains remaining from cycle 1, a secant stiffness line emerged that was quite similar to the tangent stiffness lines from both cycles.

**Fig. 8.** Case 8: (a) pile stiffness for a for a 600 mm diameter spun-pile, first cycle (data from Kim et al. (2011)); (b) pile stiffness for cycle 2 (data from Kim et al. (2011)).



### Case 9: The authors' case

The authors' static loading test was carried out in two cycles. The first cycle included five increments to about 14 MN followed by unloading. The reloading cycle went to the 14 MN load in three increments and continued with two, about 2 MN, increments to a maximum load of about 18 MN. The load-holding durations ranged from 30 min to 6 h. The authors' paper includes diagrams showing the secant modulus "*derived using elastic strain*" and the tangent modulus "*pile compressive elastic strain*", which I used to extract the authors' stress and strain values to duplicate the diagrams — here shown in Fig. 9. I understand from the paper that the two series of stress and strain values are supposed to be the same. However, the tangent modulus diagram shows that while this is so for the first five data points, the points from the 14, 16, and 18 MN load levels in the authors' secant and tangent modulus diagrams for elastic strains are plotted from different sets of values.

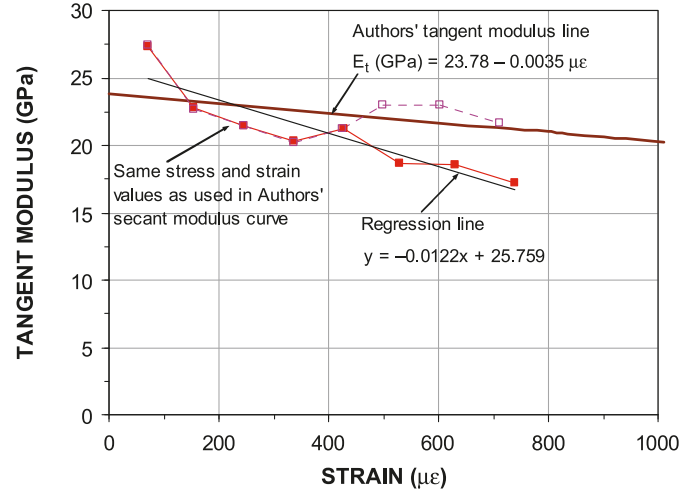
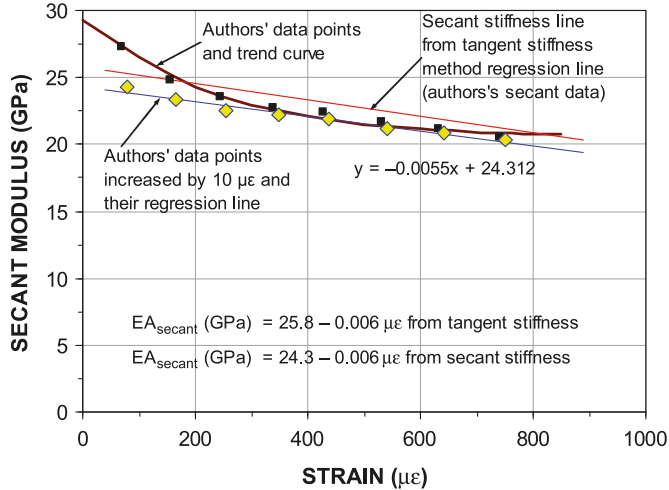
As an aside reflection, knowing how difficult it is to separate elastic and creep portions for measurements taken at each load level, in particular, when the preceding load-holding time differs between the levels, I would have expected a more scattered data plot than displayed in the authors' secant modulus curves.

More important, the secant stiffness diagram shows that when adding 10  $\mu\epsilon$  to the reported strain values (ranging from 70  $\mu\epsilon$  through 870  $\mu\epsilon$ ), the appearance of exponential shape is replaced by a linear trend secant modulus line that is quite similar to the secant modulus line determined from the tangent stiffness method.

### Conclusions

In my opinion, my eight case records and the authors' case do not support that the pile stiffness would follow an exponentially diminishing trend, with the modulus in the lower end of the strain scale being considerably larger (by 50% and more) than at the higher end of the particular range of strains imposed on test piles. The exponential trend sometimes found for the first increments of load is influenced by several factors; a few have been mentioned above. While similar influences can exist for the gages level farther down the pile, they are not likely to be the same. Nor for that matter is it assured that the gage levels farther down the pile will have the same linear dependency to strain as that determined in the secant and tangent stiffness methods (both should be used) for the uppermost gage. However, the linear dependency is about as far as it is meaningful to go. In analyzing a particular set of test data, the results of the secant and tangent

Fig. 9. Case 9. Authors' pile stiffness values (stress and strain values are from authors' paper, Figs. 9 and 10).



stiffness methods should always be reviewed in the light of what can be considered for the pile cross section at the various gage levels. The results should also be combined with the results of other methods, such as for example the direct load–strain response. Finally, as the authors demonstrated, the potential presence and effect of residual load need to be brought into the analyses before the soil response can be appraised.

## References

- Bradshaw, A.S., Haffke, S., and Baxter, C.D.P. 2012. Load transfer curves from a large-diameter pipe pile in silty soil. *In Full-scale testing and foundation design: Honoring Bengt H. Fellenius*. ASCE Geotechnical Special Publication 227. Edited by M.H. Hussein, K.R. Massarsch G.E. Likins, and R.D. Holtz. American Society of Civil Engineers, Reston, Va. pp. 590–601.
- CH2M Hill. 1995. Static loading test and analysis, Container Wharf, Berths 302 to 305, Port of Los Angeles, Los Angeles, Calif. CH2M Hill. Company report.
- Fellenius, B.H., and Tan, S.A. 2010. Combination of O-cell test and conventional head-down test. *In The art of foundation engineering practice*. ASCE Geotechnical Special Publication 198. Edited by M.H. Hussein, J.B. Anderson, and W.M. Camp. American Society of Civil Engineers, Reston, Va. pp. 240–259.
- Fellenius, B.H., Harris, D.E., and Anderson, D.G. 2004. Static loading test on a 45 m long pipe pile in Sandpoint, Idaho. *Canadian Geotechnical Journal*, **41**(4): 613–628. doi:10.1139/t04-012.
- Fellenius, B.H., Kim, S.-R., and Chung, S.G. 2009. Long-term monitoring of strain in instrumented piles. *Journal of Geotechnical and Geoenvironmental Engineering*, **135**(11): 1583–1595. doi:10.1061/(ASCE)GT.1943-5606.0000124.
- Geo Optima Pt. 2011. Instrumented loading test for Holcim Cement Plant near Tuban, East Java, Indonesia. Geo Optima Pt. Company report.
- Kim, S.R., Chung, S.G., and Fellenius, B.H. 2011. Distribution of residual load and true shaft resistance for a driven instrumented test pile. *Canadian Geotechnical Journal*, **48**(4): 583–598. doi:10.1139/t10-084.
- Lam, C., and Jefferis, S.A. 2011. Critical assessment of pile modulus determination methods. *Canadian Geotechnical Journal*, **48**(10): 1433–1448. doi:10.1139/t11-050.